Original Article

Institution of MECHANICAL ENGINEERS

Journal of ENGINEERING TRIBOLOGY

Proc IMechE Part J:
J Engineering Tribology
0(0) 1–10

DOI: 10.1177/1350650118777143
journals.sagepub.com/home/pij
SAGE

# Analysis of the conditions for the occurrence of the effect of a minimum of friction in hybrid bearings based on the load separation principle

**Roman Polyakov[1], Leonid Savin[1] and Alex Fetisov[2]**

### Abstract

Reliability of rotating machinery is determined to a considerable degree by the bearing units. For several applications the requirements in rotational speed, bearing load and maximal vibration level are so extreme that neither rolling-element bearings nor fluid-film bearings could provide necessary operating characteristics during all regimes of operation. Hybrid bearings, which are a combination of rolling-element and fluid-film bearings, can improve performance characteristics and reliability of the rotor-bearing systems. A hybrid bearing, where a rolling-element bearing and a fluid-film bearing are positioned parallel to the vector of external load (PLEX), has the following advantages compared to a single bearing, whether rolling-element or fluid-film one: increase of life expectancy, load capacity increase, friction reduction, thermal regime enhancement, increase of stiffness, and damping properties. The present paper presents the results of theoretical and numerical research of friction characteristics of PLEX in mixed sliding and rolling friction, i.e. combination of viscous and rolling contact friction, regime. The conditions of minimum friction effect occurrence have been substantiated, and rational relations between characteristics of hybrid rolling-element bearings and fluid-film bearings needed for provision of such effect have been experimentally proven. Finally, the paper presents recommendations regarding design of such hybrid bearings for heavily loaded bearing nodes of rolling mills.

### Keywords

Rolling-element bearing, fluid-film bearing, hybrid bearing, friction torque, Stribeck curve

Date received: 26 December 2017; accepted: 19 April 2018

## Introduction

Bearing nodes of rotors (rolling-element bearings, fluid-film bearings, active magnetic bearing) provide necessary characteristics of rotational motion of rotors and have dual nature in terms of their role as parts of a machine. On one hand, they have low cost in terms of total financial expenses during development of a rotor machine, except active magnetic bearing (AMB), and on the other hand,[1] unless it is an AMB,[2] they have a significant influence on the main principle of operation of a rotor machine—provision of operational process by means of rotational motion. Failure of a bearing could lead to catastrophic consequences; this is especially relevant to liquid rocket engines and aircraft engines.[3] Incorrectly designed or chosen serial bearing and violation of assembling rules lead to increased friction torque and deterioration of thermal regime of a bearing. If a failure, however, occurs, the possibility of withstanding the disturbance and retrieving the machine's regime back to normal greatly depends on the ability of bearings to operate under critical conditions. For example, if a blade is torn off of a gas turbine engine's compressor, rapid increase of imbalance occurs, with cavitational wear of a turbine's impeller uneven distribution of mass leads to the same scenario of increase of dynamic load on the bearings (Figure 1(a)). When internal combustion engine's (ICE) compressor is operating under significant temperature drop conditions, oil fouling and carbonization occur on the journal of the shaft and, consequently, imbalance changes and dynamic load increases (Figure 1(b)).

[1]Department of Mechatronics, Mechanics and Robotics, Orel State University named after I.S. Turgenev, Oryol, Russian Federation
[2]Modeling of Hydro and Mechanical Systems Research Laboratory, Orel State University named after I.S. Turgenev, Oryol, Russian Federation

**Corresponding author:**
Roman Polyakov, Department of Mechatronics, Mechanics and Robotics, Orel State University, Naugorskoye shosse 29, Oryol 302020, Russian Federation.
Email: romanpolak@mail.ru

Competitiveness in energy and transport machines development is usually provided by means of increasing rotating frequencies of pumps, expanders, compressors, etc. of the rotor machines, which leads not only to the increase in useful power, but also to the increase of energy tension of parts and nodes. If a case occurs when neither a serial rolling-element bearing could be chosen, nor a fluid-film bearing could be designed to meet the requirements of the task, nor the advisability could be shown for AMB application, an approach of combination of a fluid-film bearing and a rolling-element bearing could be used in a single node. Such approach could incorporates advantages of rolling-element bearings (low start-up friction torque, rotational stability, etc.) and those of fluid-film bearings (high damping, unlimited operational speed), and allows elimination of their disadvantages—limited operational speed of rolling-element bearings and wear at start-up and shut-down regimes of fluid-film bearings. AMB systems, which given correct design are also free from the mentioned disadvantages, are, nevertheless, much more expensive.

The interest in the hybrid bearings arose in the 1960s–1970s.[4,5] In 1980s, NASA launched several research programs on hybrid hydrostatic/ball bearings for cryogenic turbopumps.[6,7] These studies demonstrated the benefits of hybrid bearings and feasibility of their use in turbomachinery applications.

There are two fundamentally different configurations of hybrid bearings. According to the abbreviations in Butner and Murphy[6] these configurations are called parallel load (PL) and parallel speed (PS). Figure 2(a) shows the latter concept of the hybrid bearing with speed separation. In this diagram, a fluid-film bearing (FFB) can be mounted on the outer race (PSEX bearing) of the rolling-element bearing (REB). Such configuration allows to reduce the rotation speed of the rolling-element bearing to a fraction of the shaft speed.[8] A rotor shaft rotates in a rolling-element bearing during start-up and shutdown. A fluid-film bearing switches on at the main operating regime. As rotation speed (and hydrostatic pressure) increases, the load capacity of the fluid-film bearing increases and the rolling-element bearing becomes partially switched off. So, life expectancy of REB is improved due to smaller DN value (product of rotation speed and shaft diameter).[8]

The PL concept shown in Figure 2(b) is referred to as a hybrid bearing with load separation. A rolling-element bearing and a fluid-film bearing are combined here in an array. Though the shaft rotates in a rolling-element bearing permanently, life expectancy of REB increases due to smaller loads at high speeds.[9,10] A rolling-element bearing carries the external load during start-up and shutdown. At the main operating mode, a fluid-film bearing discharges the rolling-element bearing due to the hydrodynamic reaction forces of the fluid film. The fluid-film bearing in this case has a guaranteed gap and thus experiences no wear during start-up and shutdown regimes.

Such principle of operation of hybrid bearings with load separation provides the following characteristics enhancements to the whole bearing node:[9–12]

1. *Provision of a wear-free regime for fluid-film bearings*. It is designed so, that the initial gap of a fluid-film bearing is guaranteed to provide the hydrodynamic lubrication regime and to counteract the external load.
2. *Increase of the rolling-element bearing's life expectancy*. Discharge of the REB due to the hydrodynamic reaction forces in the FFB leads to the increase of its and the whole node's life expectancy, since the life expectancy of a FFB in the hydrodynamic regime is unlimited.
3. *Increase of the load capacity of a bearing node* is developed due to distribution of external load over the housing simultaneously through the rolling elements and the fluid film.
4. *Increase of speed limitations of a bearing compared to a single REB*. This effect could be explained with the fact that with the increased load capacity of a bearing, a lighter or smaller REB could be used.

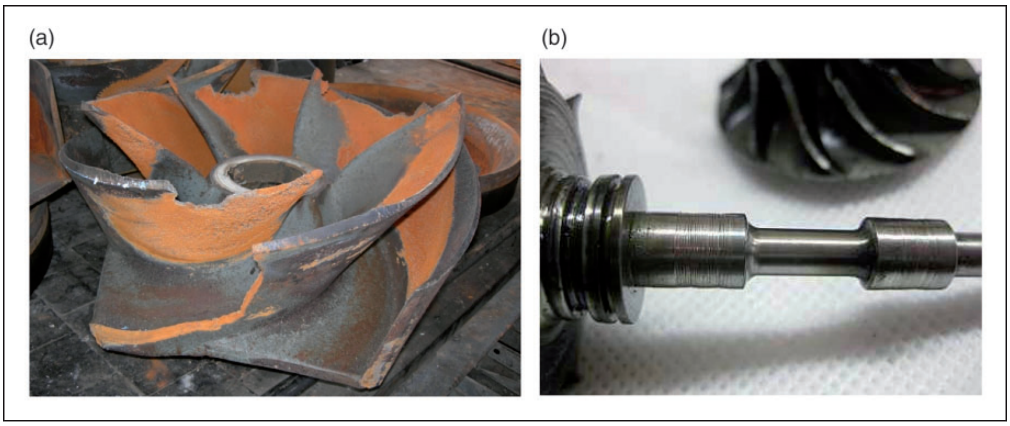


**Figure 1.** Damage to elements of rotor machines.

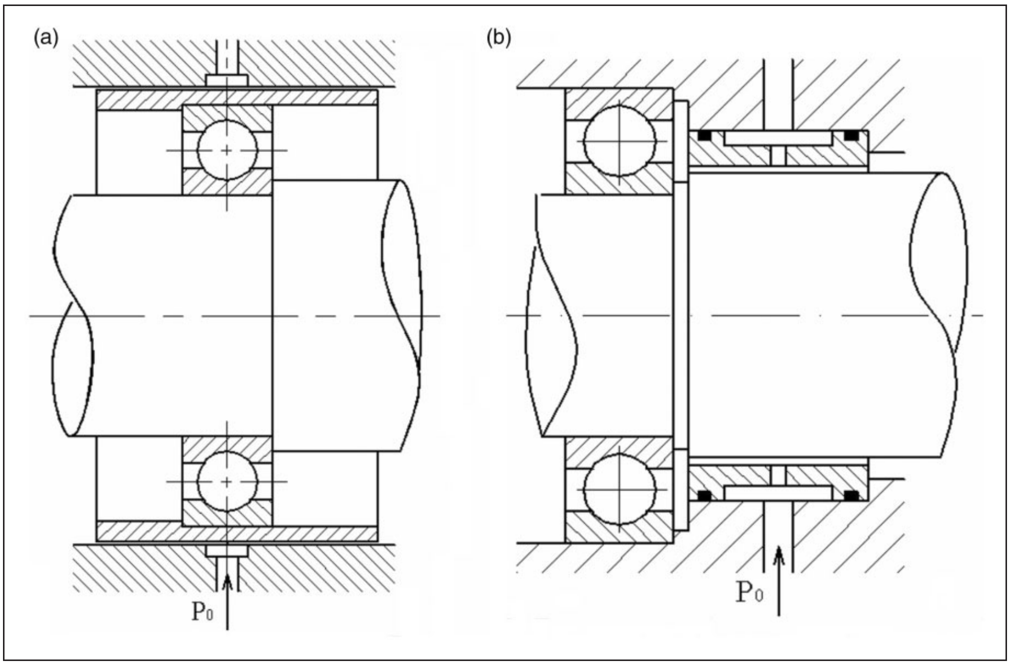


**Figure 2.** Basic hybrid bearing configurations: (a) with speed separation (PSEX) and (b) with load separation (PLEX).

5. *Decrease of the friction torque in a bearing.* Under certain conditions and combinations of operational and geometric parameters of a bearing it is possible that the total friction torque of a PLEX bearing is less than the friction torque of a single REB.
6. *Increase of stiffness of a bearing* is achieved by means of distribution of external load over the housing simultaneously through the rolling elements and the fluid film.
7. *Improvement of dynamic characteristics of a bearing* in comparison to a single REB due to significant damping effect of the fluid film of a FFB.
8. *Enhancement of the lubrication and thermal regimes* of a REB due to the presence of a lubricant supply system.

In experimental studies of some authors,[4,9,13,14,15,16] the results are shown for cases of mixed friction in the PLEX bearings that show quite complex processes of friction when the rolling friction is combined with the sliding friction, and that show that there remains a minimum of friction coefficients even with the increase of friction pairs. In Polyakov et al.,[9,11] a general substantiation of the effect of the decrease of friction is presented; however, there are no relations derived and no cases of conditions have been presented as to when this effect could occur.

In the present paper, the mechanism of occurrence of the effect of minimum friction is described in more detail, and the criteria and conditions of this effect's occurrence are determined for a case of mixed friction with accompanying results of numerical and experimental studies.

## Mathematical modeling and numerical results

Mathematical model of a PLEX bearing is based on combination of models of a radial-thrust roller-element bearing and a fluid-film bearing.

Mathematical model of a radial-thrust REB (Figure 3(a)) is based on solution of a Hertz contact problem[14,16] with the following expression for normal stress in the contact between the rolling element and the bearing's race

$$\sigma = \frac{3F_{\sum}}{2\pi ab}\left[1-\left(\frac{x}{a}\right)^2-\left(\frac{x}{a}\right)^2\right]^{1/2} \tag{1}$$

where $a$, $b$ are the major and minor semiaxes of the ellipse of the contact (Figure 3(b)); $F_{\sum}$ is the equivalent compressive force in the REB.

And surface friction shear stress

$$\tau_N = \eta\frac{v}{h} \tag{2}$$

where $\eta$ is the dynamic viscosity of fluid; $v$ is the sliding velocity; $h$ is the plateau lubricant film thickness.

As it has been shown in Harris,[16] the friction force in the contact between the rolling element and the race of the bearing could be determined as follows

$$\begin{aligned} F_{fr}^{REB} = ab\int_{-1}^{+1}\int_{-\sqrt{1-q^2}}^{+\sqrt{1-q^2}} c_v\frac{A_c}{A_0}\mu_a\sigma \\ +\left(1-\frac{A_c}{A_0}\right)\left(\frac{1}{\tau_N}-\frac{1}{\tau_{lim}}\right)dtdq \end{aligned} \tag{3}$$

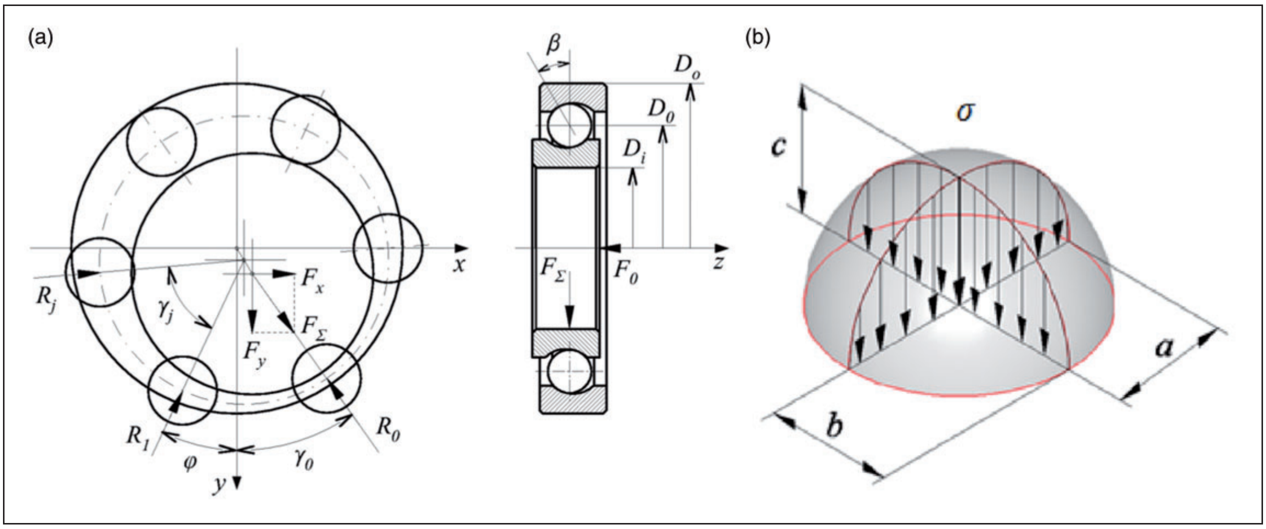


**Figure 3.** (a) Diagram of a radial-thrust roller-element bearing and (b) the pressure distribution in the contact.

where $A_c$ is the true average contact area; $A_0$ is the apparent contact area; $\mu_a$ is the asperity–asperity friction coefficient; $\tau_{lim}$ is the limiting shear stress in fluid.

And to analyze the characteristics of a bearing, it is convenient to use the following parameters of friction torque and power loss due to friction

$$M_{fr}^{REB} = F_{fr}\frac{D_0}{2} \tag{4}$$

$$N_{fr}^{REB} = M_{fr}\omega \tag{5}$$

So, the friction torque of a REB could be divided into two components—the one that depends on the compressive stress $M_{fr}\,(F_{\sum})$ and the one that depends on the sliding velocity $M_{fr}(\omega)$ as follows

$$M_{fr}^{REB} = M_{fr}^{REB}\left(F_{\sum}\right) + M_{fr}^{REB}(\omega) \tag{6}$$

Mathematical model of a hydrodynamic bearing is based on the equations of hydrodynamic lubrication theory.[17–19] Determination of reaction forces of a plain hydrodynamic or a hydrostatic bearing with point orifices is based on the integration of pressure distribution $p(x, z)$ over the bearing's surface, which is determined from the numerical solution of the Reynolds equation

$$\frac{\partial}{\partial x}\left[\frac{\rho h^3}{\mu K_x}\frac{\partial p}{\partial x}\right] + \frac{\partial}{\partial z}\left[\frac{\rho h^3}{\mu K_z}\frac{\partial p}{\partial z}\right] = 6\frac{\partial}{\partial x}(\rho U h) - 12\rho V \tag{7}$$

where $p$ is the unknown function of pressure distribution; $x = \phi R$ is the circumferential coordinate; $z$ is the axial coordinate (Figure 3(a)); $h$ is the radial gap function: $h = h_0 - X\sin\alpha - Y\cos\alpha$; $\rho, \mu$ are the density and dynamic viscosity of a lubricant; $K_x$, $K_z$ are the turbulence coefficients along the $x$ and $z$ coordinates accordingly; $U$ is the velocity distribution in the circumferential direction.

$$U = \frac{\omega D}{2} - \dot{X}_0 \sin\frac{2x}{D} + \dot{Y}_0 \cos\frac{2x}{D} \tag{8}$$

$V$ is the velocity distribution in the radial direction on the surface of the journal

$$V = \dot{X}_0 \cos\frac{2x}{D} + \dot{Y}_0 \sin\frac{2x}{D} \tag{9}$$

Here, $\omega$ is the angular velocity of a rotor; $\dot{X}_0$ and $\dot{Y}_0$ are the velocities of the journal's center in the $XOY$ coordinates; turbulence coefficients $K_x$ and $K_z$, that take the change of effective viscosity due to turbulence occurrence into account, and that could be determined using the Constantinesku's method[20]

$$K_x = 1 + 0.044(k^2 Re)^{0.725}; \quad K_z = 1 + 0.0247(k^2 Re)^{0.65} \tag{10}$$

where $Re$ is the local Reynolds number and $k$ is the Karman coefficient.

Friction torque of a FFB depends mostly on the sliding velocity

$$M_{fr}^{FFB} = M_{fr}^{FFB}(\omega) = -\frac{D}{2}\int_0^L \int_0^{\pi D} \tau \sin\alpha \, dx\, dz \tag{11}$$

$$\tau = \frac{h}{2}\frac{\partial p}{\partial x} + \frac{\mu U}{h} \tag{12}$$

So, the friction torque of a FFB depends on the velocity, and the total friction torque of the PLEX could be determined as a sum of the friction torques of the combined bearings

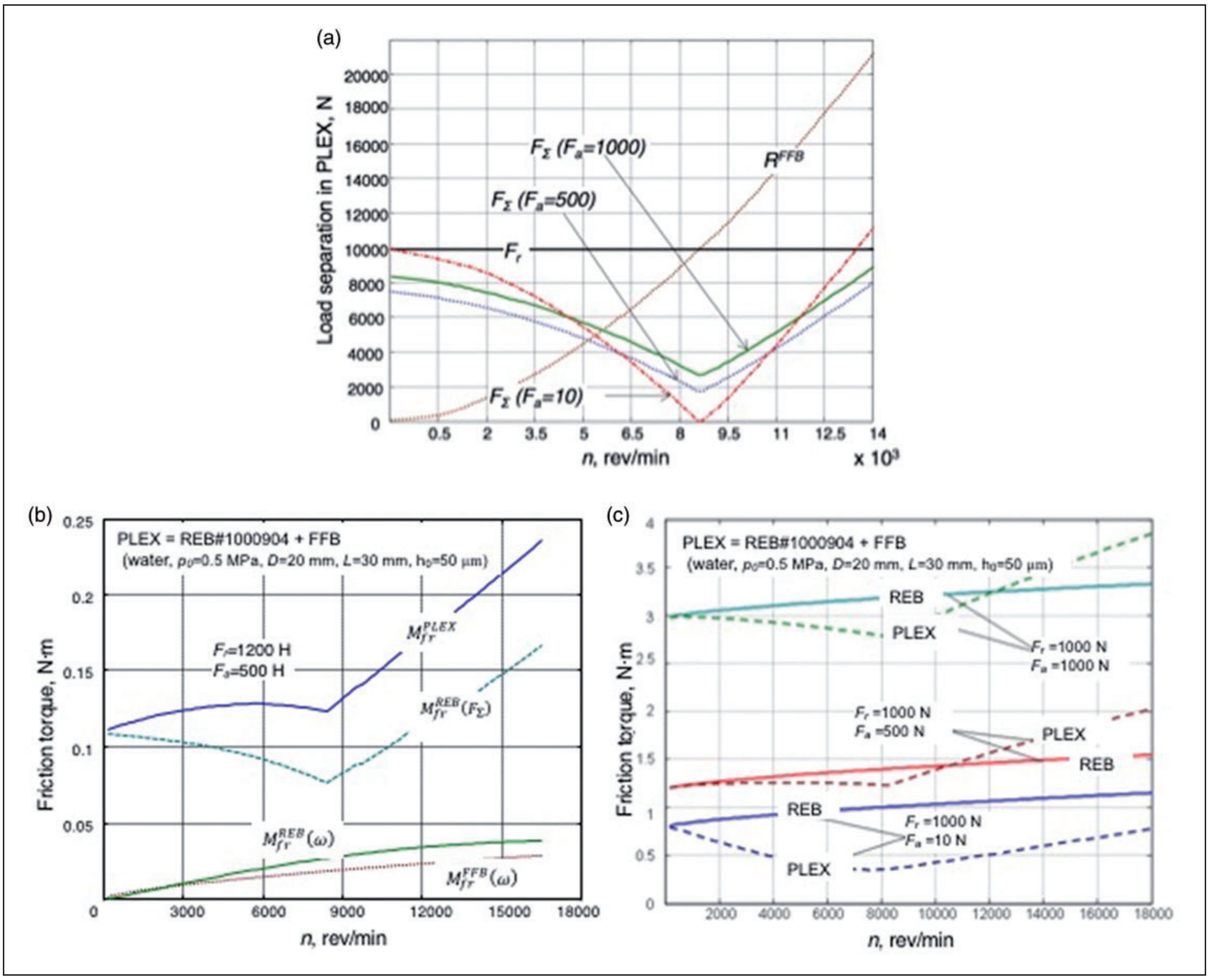


**Figure 4.** Total friction torque of a PLEX bearing and its components.

$$M_{fr}^{PLEX} = M_{fr}^{REB}\left(F_{\sum}\right) + M_{fr}^{REB}(\omega) + M_{fr}^{FFB}(\omega) \tag{13}$$

Figure 4 shows the dependency of the total friction torque of the PLEX and its components on the rotational velocity. Here, if the velocity is such that the radial load on a REB and a FFB is equal (Figure 4(a)), some decrease in the total friction torque could be seen for a PLEX bearing. The magnitude of this decrease is then bigger, when the component of the total friction torque that depends on the load $M_{fr}^{REB}(F_{\sum})$ has more influence.

The given results are obtained given the following parameters of the rotor system: PLEX is composed of a rolling-element radial-thrust bearing No. 1000904 ($D_i = 20\,\text{mm}$, $D_e = 37\,\text{mm}$, i = 10, $d_w = 5\,\text{mm}$) and a hydrodynamic fluid-film bearing ($D = 20\,\text{mm}$, $L = 30\,\text{mm}$, $h_0 = 50\,\mu\text{m}$, $p_0 = 0.5\,\text{MPa}$, lubricant–water); equivalent radial load on a single PLEX bearing is 1000..10000 N, axial load on a single PLEX is 10..1000 N.

So, given a certain combination of operational parameters, it could be seen, that the total friction torque of the PLEX bearing could be less than the friction torque of a single REB (Figure 4(b)), which is then bigger, when the external load is higher (Figure 4(c)). In other words, during the development stage of the PLEX bearing design the parameters could be chosen so, that not only the life expectancy of the bearing is longer, but also the friction torque is less than one of a single REB.

It could be seen from Figure 4(c) that with the increase of the axial load the effect of decrease of the total friction torque is leveled due to the increase in the number of rolling elements that take part in counteracting the load and due to the increase in the component of the total friction torque that greatly depends on the axial load.

As it could be seen, in the area of full unloading depending on the radial to axial load ration different manifestation of the effect of minimum friction could be observed. Maximum rate of decrease in friction torque could be obtained with $F_a/F_r \to 0$, but it is noted in Harnoy[14] and Harris[16] that

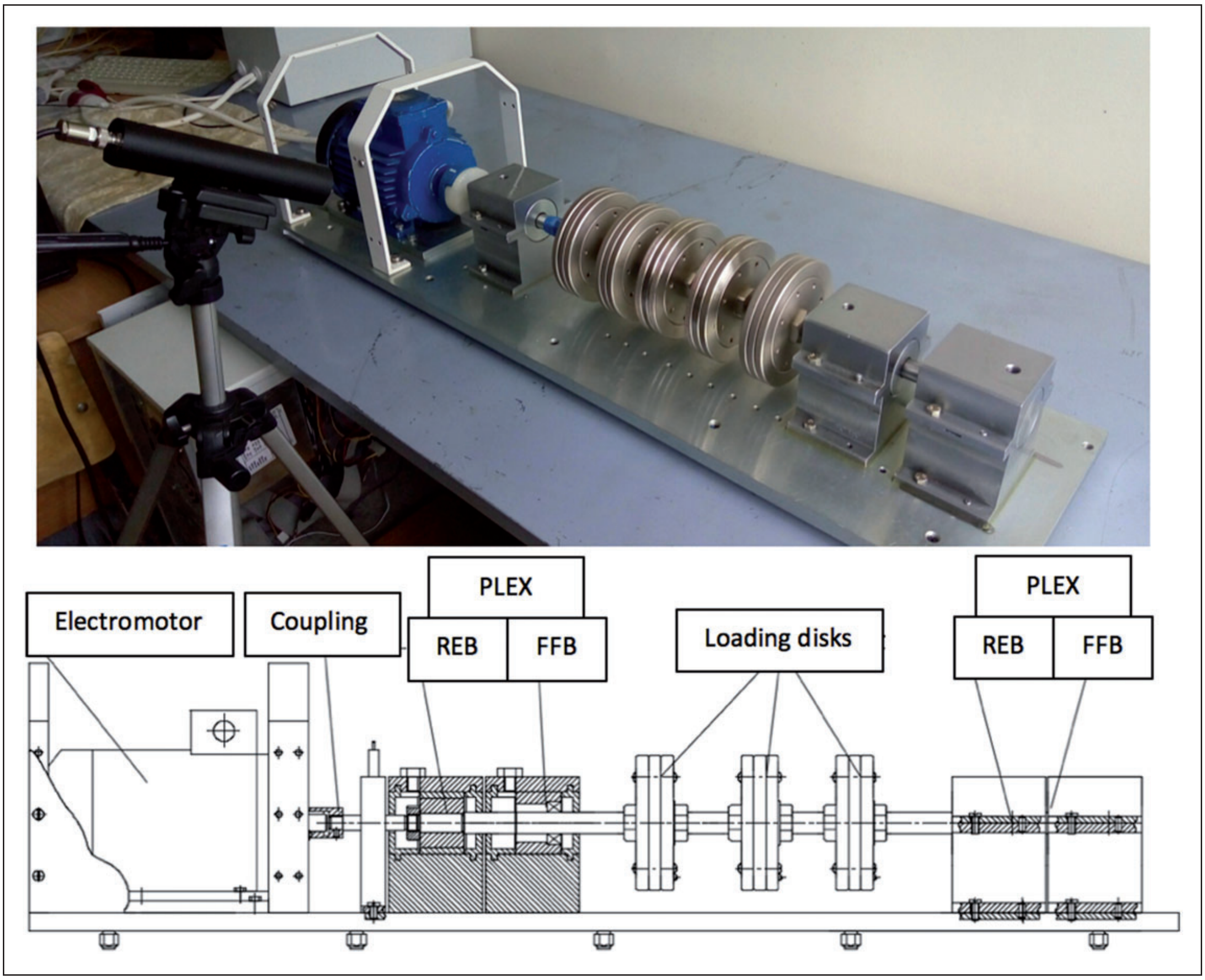


**Figure 5.** Test rig with PLEX bearings.

operation of REB without preload causes fewer rolling elements to get into contact and carry the external load, and slip of the rolling elements to occur. Also, the effect of stiffness drop described in Polyakov et al.[21] might occur during the unloaded regime in a PLEX, which happens due to the decrease of the deformation level of the rolling elements and the decrease of the equivalent stiffness of a bearing.

## Experimental studies

To study the presented effect a series of experiments has been carried out using a developed test rig (Figure 5) using a single REB and with a REB together with a hydrodynamic FFB for one case and together with a FFB with point orifices for another case.

The parameters of the studied bearings and levels of their variation are presented in Table 1. The methodology of the tests implied the rotor's acceleration to the rotation velocity higher than the one that corresponds to the effect of maximum unloading, and acquirement of the rotor's run-out. According to the conservation of the kinematic torque law during the run-out

$$J\frac{\mathrm{d}\omega}{dt} = M_{fr}^{PLEX} \tag{14}$$

where $J$ is the polar inertia torque of the rotor and $\omega$ is the angular velocity of the rotor.

Inertia torque was determined numerically using the Solid Works software. So, knowing $d\omega/dt$ one could estimate the friction torque.

Knowing the friction torque and the relation between the angular velocity and the run-out duration, one could estimate the friction coefficient using the method described in Chikhos[22] as the ratio between the friction force and the applied force

$$M_{fr}^{PLEX} = F_{ext}\frac{D}{2} \tag{15}$$

**Table 1.** Test rig parameters.

| NO. | Parameter | Variation range |
|---|---|---|
| 1 | Rolling-element bearing | #203: $d = 17$ mm, $D = 35$ mm, $B = 11$ mm |
| 2 | Fluid-film bearing | $D = 40$ mm, $L = 36$ mm, $h_0 = 300$ μm, lubricant: oil I12 ($\mu_0 = 0.01$ Pa·s), relative eccentricity: 0.33..0.66 |
| 3 | Rotation velocity, $n$ | 0. . .1000, r/min |
| 4 | Imbalance, $m\Delta$ | $4 \times 10^{-6}$ kg·m |
| 5 | Static load (mg) | |
| | – shaft with 1 disk ($m = 3.14$ kg) | 30.77 N |
| | – shaft with 2 disk ($m = 5.25$ kg) | 51.45 N |
| | – shaft with 3 disk ($m = 7.35$ kg) | 72.03 N |
| | – shaft with 4 disk ($m = 9.46$ kg) | 92.70 N |
| | – shaft with 5 disk ($m = 11.57$ kg) | 113.38 N |
| 6 | Axial inertia torque (J) | |
| | – shaft with 1 disk | 0.0038 kg·m$^2$ |
| | – shaft with 2 disk | 0.0076 kg·m$^2$ |
| | – shaft with 3 disk | 0.0113 kg·m$^2$ |
| | – shaft with 4 disk | 0.0151 kg·m$^2$ |
| | – shaft with 5 disk | 0.0189 kg·m$^2$ |

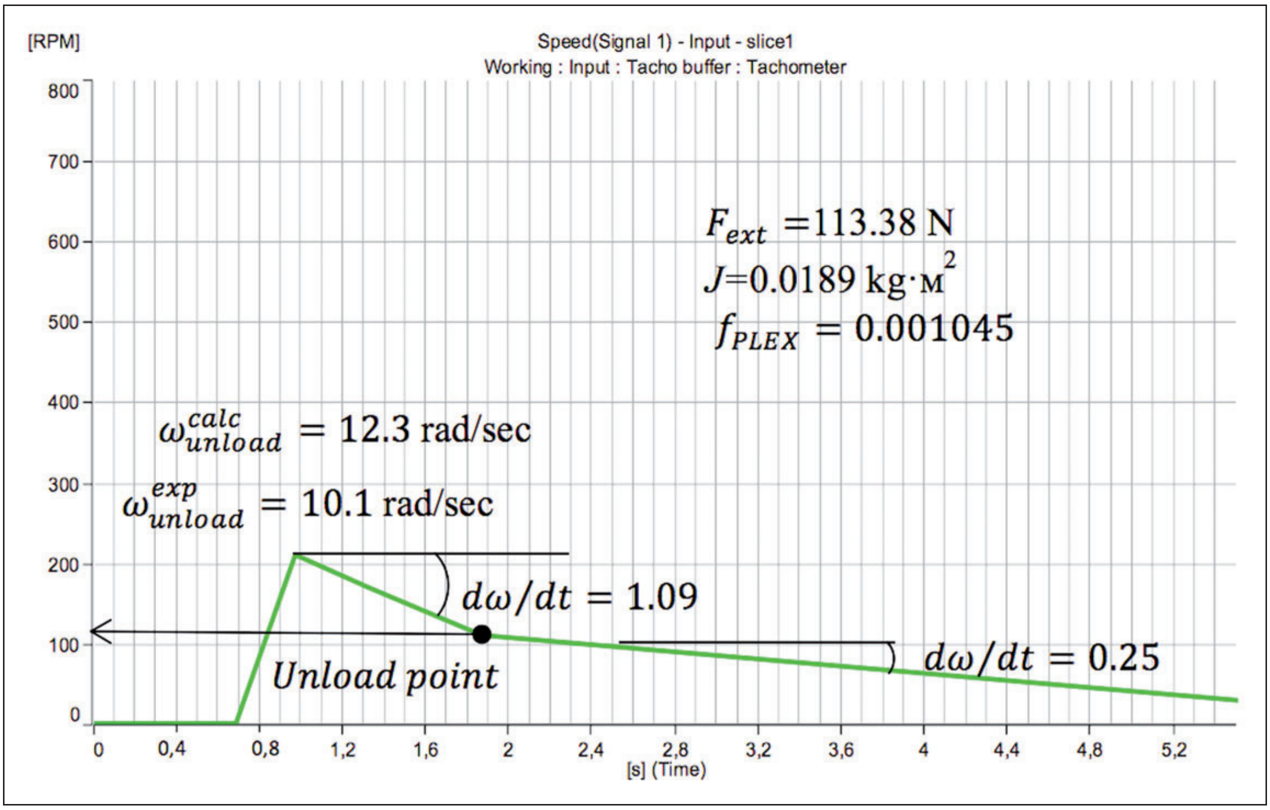


**Figure 6.** Run-out curves of a rotor on PLEX bearing with a hydrodynamic FFB.

$$f = \frac{2J\frac{d\omega}{dt}}{F_{ext}D} \tag{16}$$

In Figure 6, the characteristic diagram of the rotor's run-out on PLEX bearings is presented, which shows the decrease in friction after the unloading of the rotor. When the run-out starts (approx. starting from the first second) until 1.88 s the slope of the run-out curve, characterized by the derivative $d\omega/dt$ has a value of 1.09, and after this moment the effect of unloading occurs, and the friction coefficient decreases by approximately four times. Here, the calculated angular velocity was 12.3 rad/s and the experimentally determined velocity was 10.1 rad/s. This 18% deviation could be explained by the additional displacement of the rotor to the area of higher eccentricity in the FFB due to the elastic flexure of the shaft's axis and full unloading of the REB at lower value of angular velocity than the calculated value.

According to equation (16), the friction coefficient of the PLEX bearing during unloading for two similar bearings could be determined as follows

$$F = \frac{2J\frac{d\omega}{dt}}{F_{ext}D} = \frac{2 \cdot 0.0189 \cdot 2.5}{113 \cdot 0.04} = 0.0209$$

For one bearing $f_{PLEX} = 0.01045$, it matches the numerical and experimental data of other authors.[1,6,7,10,12]

It should be noted that in Butner and Murphy,[6] it is shown that for a PLEX bearing with a hydrostatic FFB the effect of decrease of friction does not occur due to the fact that the hydrostatic bearing is mounted coaxially with the rolling-element bearing, and owing to the small deformations of the rolling elements, the hydrostatic effect of unloading is negligibly small, but here the component of friction is added, which occurs due to viscous friction. For the effect of unloading to occur in a PLEX bearing with a hydrostatic FFB, either the eccentricity has to be artificially manipulated, or the feeding orifices have to be distributed unevenly over the surface of the bearing. This in its turn leads to the necessity of development of a new simulation model and requires additional research.

Figure 7 shows the dependency of the total friction coefficient of the PLEX bearing on the dimensionless Sommerfeld number:[23] a hydrodynamic bearing mounted coaxially with a rolling-element bearing (curve 1) and mounted eccentrically relative to the axis of the REB (curve 2). It is clear that the friction coefficient drops about 15% during the unloading of the REB.

The curve shows the following advantages of combined FFB and REB with load separation: absence of dry and boundary friction regimes, lower friction coefficient during the main operational regime of PLEX bearings, more shallow curve representing the friction increase.

As it is noted in Polyakov et al.,[21] such effect is not observed in a combination of a REB and a hydrostatic bearing due to the throttling effect.

So, four conditions could be highlighted for minimum friction effect occurrence in hybrid bearings with load separation principle:

1. The reaction force of a fluid-film bearing needs to be as close to the load in terms of value and direction as possible.
2. Relatively stable position of a rotor in a fluid-film bearing—eccentricity deviation should not exceed 10% of the radial gap.
3. Value of the axial load should not exceed 5% of the radial load.

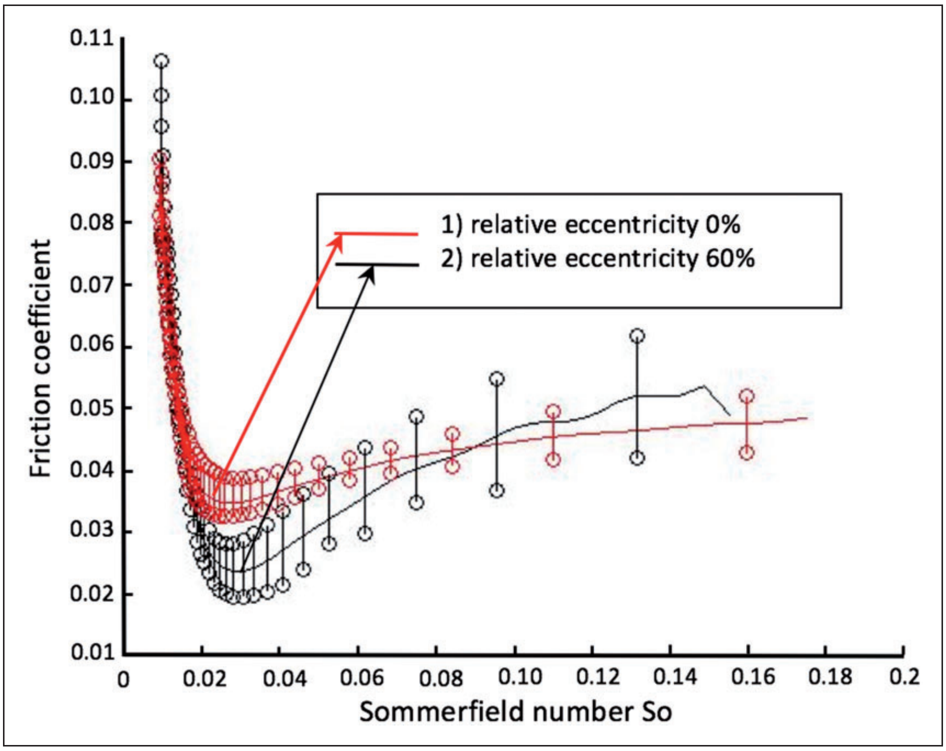


**Figure 7.** Friction decrease effect during the unloading of the PLEX bearing.

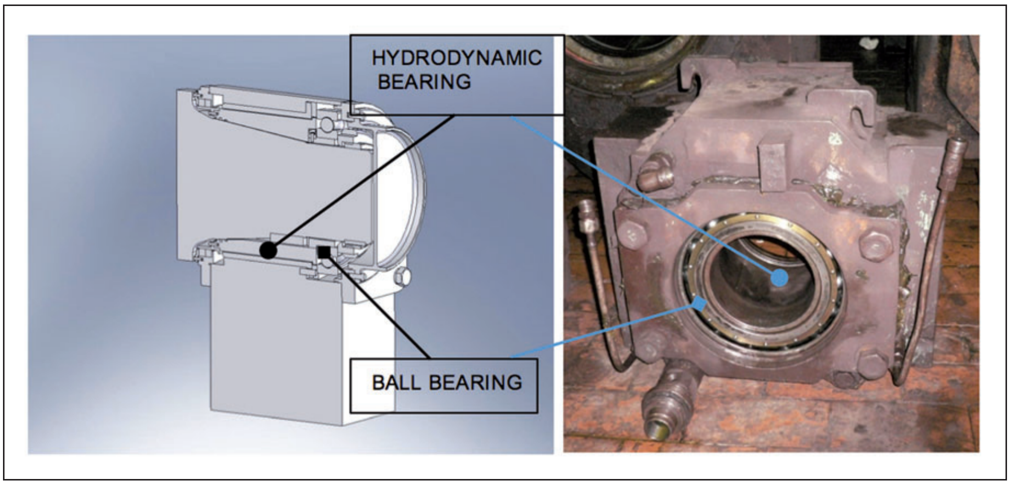


**Figure 8.** PLEX bearing of a roller of a rolling mill.

4. Value of the radial load of a fluid-film bearing should be at least 60% of dynamic load capacity.

Even such small decrease of the friction coefficient during the steady-state regime could lead to great advantages in terms of the whole life span of a rotor-bearing node, and could significantly decrease the cost of energy at a scale of a whole industrial institution.

One of the most promising fields of application of PLEX bearings are rolls of the rolling mills. In Figure 8(a), PLEX bearing of a SKET rolling mill[24] is presented, which consists of a radial-thrust doubled roller bearing and a radial hydrodynamic bearing. Evaluation of possibility of power loss due to friction decrease has shown that during the steady-state regime there is a decrease up to 0.7 kW, which is a considerable saving in terms of energy consumption.

During simulation the following parameters were used:

1. Lubricant: oil MS-20 (density $\rho = 900\,\text{kg/m}^3$, dynamic viscosity $\mu = 0.018\,\text{Pa·s}$);
2. Lubricant supply flow rate: 21.6 $\text{m}^3$/h;
3. Inlet pressure: 0.15 MPa;
4. Power of the motor: 6.00 kW;
5. Rotational speed: 145...492 r/min;
6. Acceleration (deceleration) time: 4 s;
7. Number of shut-downs: 5...8 per day;
8. Guaranteed life expectancy: 10,000 h;
9. Maximum load during the rolling process: $F_r \approx 270$ kN, $F_a \approx 0$ N;
10. Mass of the rotor: 0.75 t.

Parameters of the REB: 46330 series radial-thrust bearing, $C_D = 357\,\text{kN}$, $C_D = 370\,\text{kN}$. Parameters of the FFB: diameter $D = 154\,\text{mm}$; length $L = 140\,\text{mm}$; radial gap $h = 77\,\mu\text{m}$.

So, it has been shown theoretically and experimentally that the combination of a REB and a FFB according to the load separation principle leads to a decrease of friction effect's occurrence in a rotor-bearing node. Given all other parameters equal, one could achieve an up to 45% decrease of friction depending on the radial and axial load. Moreover, unloading of a REB during the steady-state regime and the guaranteed value of the radial gap leads to the significant increase of life expectancy of the hybrid bearing. PLEX bearings could be successfully applied in highly loaded bearing nodes that operate under low rotational speeds, such as rollers of rolling mills used in metallurgical production, and low-speed turbines of energy generators.

## Declaration of Conflicting Interests

The author(s) declared no potential conflicts of interest with respect to the research, authorship, and/or publication of this article.

## Funding

The author(s) disclosed receipt of the following financial support for the research, authorship, and/or publication of this article: This work was supported by the Ministry of Education and Science of the Russian Federation under Project no. 9.2952.2017/4.6 (development and modernization of the test rig) and by the Russian Science Foundation under Project no. 16-19-00186 (formulation and solution of the problem in all sections of the present paper).

## References

1. Olaru P. Nano-soldering pseudo-composite material to decrease engine bearing failure. In: *16th EDF-PPRIME Workshop Poitiers – FUTUROSCOPE, Behaviour of journal and thrust bearings under transient and mixed lubrication regime*, France, 2017, pp.17–18.
2. Beschastnih VN and Ravikovich YA. Gas bearing of heavy rotor of gas turbine engines. Experience in development and implementation prospects. *Vestnik Moskovskogo Aviatsionnogo Instituta* 2010; 17: 91–98.
3. Belousov AI and Gritsin AV. Gas turbine engine disk risk assessment at the design state taking into account random failures. *Russian Aeronaut* 2013; 56: 359–364.

4. Hanovich MG. *Fluid-film bearings and hybrid bearings*. Leningrad: Mashgiz, 1960.
5. Parker RJ, Fleming DP, Anderson WJ, et al. Experimental evaluation of the series-hybrid rolling-element bearing. NASA TN D-7011, 1970, 27 pp.
6. Butner MF and Murphy BT. Space shuttle main engine long-life bearings. NASACR179455, 1986, 163 pp.
7. Nielson CE. Hybrid hydrostatic/ball bearings in high-speed turbomachinery. NASA CR-168124, 1982, 386 pp.
8. Anderson WJ, Fleming DP and Parker RJ. The series hybrid bearing - a new high speed bearing concept. *ASME J Lubr Technol* 1972; 94: 117–124.
9. Polyakov RN. *Improving of dynamics and working life of rotor supports by coupling rolling-element and fluid-film bearings*. Doctoral Thesis, Orel State Technical University, Russia, 2005, 154 pp.
10. Polyakov RN, Pugachev AO and Savin LA. Vibration reduction in rotor systems on hybrid hydrostatic/ball bearings with load separation. In: *9th international conference on motion and vibration control*, 2008, p. 90.
11. Polyakov RN, Pugachev AO and Savin LA. Reliability improvement of rotor supports by combining rolling-element bearings and fluid-film bearings. In: *7th EDF/LMS Poitiers Workshop FUTUROSCOPE, Operational limits of bearing: Improvement of performance trough modeling and experimentation*, 2008, pp.K1–K8.
12. Polyakov RN, Savin LA and Shutin DV. Reliability improvement of rotor supports by combining rolling-element bearings and fluid-film bearings. *Appl Mech Mater* 2014; 630: 188–198.
13. Harnoy A. *Composite bearing-rolling element with hydrodynamic journal*. MS Thesis, Technion – Israel Institute of Technology, Israel, 1966.
14. Harnoy A. *Bearing design in machinery: Engineering tribology and lubrication*. New York: Marcel Dekker, Inc, 2003, p.640.
15. Pietsch E. Zur Frage der Kombination von Gleit-und Wälzlagern. Maschinenbautechnik, 5, 1956.
16. Harris TA. *Rolling bearing analysis*. 5th ed. New York: Wiley-Interscience, 2006.
17. Cameron A. *Basic Lubrication Theory*. Longman Group Ltd., London. 1971.
18. Khonsari MM and Booser ER. *Applied Tribology: Bearing Design and Lubrication*. New York : John Wiley. 2001.
19. Szeri A. *Fluid film Lubrication: Theory and Design*. Cambridge University Press, Cambridge. 2005.
20. Constantinescu V. Basic relationships in turbulent lubrication and their extension to include thermal effects. *Trans ASME, Ser F* 1973; 2: 35–43.
21. Polyakov R, Savin L and Shutin D. Reliability improvement of rotor supports by combining rolling-element bearings and fluid-film bearings. *Appl Mech Mater* 2014; 630: 188–198.
22. Chikhos K. *System Analysis in Tribotechnics*. Mir Publ., Moscov. 1982.
23. Shigley JE and Mischke CR. *Mechanical engineering design*. New York: McGraw-Hill, 1989.
24. Allgemeiner Maschinenbau und Windenergieanlagenbau, www.sket.de (accessed 1 October 2017).

## Appendix

### *Notation*

| | |
|---|---|
| $a$, $b$ | major and minor semiaxes of the ellipse of the contact |
| $A_c$ | true average contact area |
| $A_\sigma$ | apparent contact area |
| $d_w$ | diameter of rolling elements |
| $D$ | diameter of FFB |
| $D_i$ | internal diameter of REB |
| $D_e$ | external diameter of REB |
| $D_0$ | average diameter of REB |
| $F_a$ | axe force |
| $F_r$ | radial force |
| $F_{\sum}$ | equivalent compressive force |
| $F_f^{REB}r$ | friction force of a REB |
| $h_0$ | average bearing gap |
| $h = h_0 - Xsin\alpha - Ycos\alpha$ | radial gap function |
| $i$ | number of rolling elements |
| $J$ | polar inertia torque of the rotor |
| $k$ | Karman coefficient |
| $K_x$, $K_z$ | turbulence coefficients along the x and z coordinates accordingly |
| $L$ | length of FFB |
| $m_\Delta$ | imbalance |
| $M_{fr}^{FFB}$ | friction torque of a FFB |
| $M_{fr}^{REB}$ | friction torque of a REB |
| $n$ | rotation velocity |
| $p_0$ | fluid flow pressure |
| $Re$ | local Reynolds number |
| $U$ | velocity distribution in circumferential direction |
| $V$ | velocity distribution in the radial direction on the surface of the journal |
| $x = \phi R$ | circumferential coordinate |
| $X$, $Y$ | displacements of the journal's center in the $XOY$ coordinates |
| $\dot{X}_0$ and $\dot{Y}_0$ | velocities of the journal's center in the XOY coordinates |
| $z$ | axial coordinate |
| $\alpha$ | angular coordinate along the bearing surface, defining the radial clearance |
| $\beta$ | angle of contact in rolling element bearing |
| $\mu_a$ | asperity–asperity friction coefficient |
| $\nu$ | sliding velocity |
| $\omega$ | angular velocity of a rotor |
| $\rho$, $\mu$ | density and dynamic viscosity of a lubricant |
| $\sigma$ | normal stress in the contact between the rolling element and the bearing's race |
| $\tau_{lim}$ | limiting shear stress in fluid |